

A quantitative co-localization analysis of large unspliced tenascin-C_L and laminin-5/γ2-chain in basement membranes of oral squamous cell carcinoma by confocal laser scanning microscopy

Marcus Franz¹, Torsten Hansen¹, Laura Borsi², Christiane Geier¹, Peter Hyckel³, Peter Schleier³, Petra Richter¹, Annelore Altendorf-Hofmann⁴, Hartwig Kosmehl⁵, Alexander Berndt¹

¹Institute of Pathology, Friedrich Schiller University of Jena, Jena, Germany; ²Istituto Nazionale per la Ricerca sul Cancro, Genoa, Italy; ³Clinic of Maxillofacial Surgery, Friedrich Schiller University of Jena, Jena, Germany; ⁴Tumour Registry, Friedrich Schiller University of Jena, Jena, Germany; ⁵Institute of Pathology, HELIOS-Klinikum, Erfurt, Germany

BACKGROUND: A structural interaction of the oncofetal large tenascin-C splice variants (Tn-C_L) and the γ2-chain of laminin-5 (Ln-5/γ2) was recently demonstrated in oral squamous cell carcinoma (OSCC). *In situ* different patterns of co-localization and co-deposition of both proteins could be detected. Especially the co-localization in re-established basement membrane (BM) structures seemed to be biologically meaningful within the process of tumour progression.

METHODS: The amount of Tn-C_L incorporated in reorganized OSCC BM structures at the tumour margins was investigated by a laser scanning microscopy-based quantitative co-localization analysis.

RESULTS: In the BM of normal oral mucosa no Tn-C_L could be detected. In dysplastic and neoplastic oral mucosa a distinct co-localization of Tn-C_L and Ln-5/γ2 in the BM region could be observed. The extent of Tn-C_L arrangement into reorganized BM structures correlated with malignancy grade.

CONCLUSIONS: The results suggest at first, a modulation of carcinomatous BM structures by the inclusion of oncofetal matrix proteins during tumour progression and secondly, the BM incorporation of the adhesion-modulating molecule Tn-C_L as a pre-invasive structural phenomenon in OSCC.

J Oral Pathol Med (2007) 36: 6–11

Keywords: basement membrane; co-localization; laminin-5; malignancy grading; oral squamous cell carcinoma; tenascin-C_L

Introduction

Changes in the composition of the extracellular matrix (ECM) influence invasion and metastasis as important processes during carcinoma progression. In oral squamous cell carcinoma (OSCC) invasion-associated alterations in the structural composition of basement membranes (BM) and changes in the qualitative protein content have been described. Only little is known about the quantitative variations of BM proteins. Among the investigated BM-related molecules, Tn-C_L and Ln-5 seem to play a certain role in OSCC.

Laminins (Ln) are heterotrimeric glycoproteins of the ECM consisting of an α-, β- and γ-chain. Sixteen distinct Ln isoforms have been described with different tissue- and development-specific functions (1–4). Ln-5 (α3β3γ2) is a constituent of the epithelial adhesion complex and connects the BM with the hemidesmosome of the cell (5, 6). It is unique among the Lns as it contains the β3- and γ2-chains (5, 7–10). In OSCC, Ln-5 shows an increased cytoplasmic accumulation, a deposition in the stroma close to budding tumour cells and is diminished in the BM at the deep invasive margins. The accumulated γ2-chain has been suggested to induce cancer cell migration (3, 11, 12). So an Ln-5-guided tumour invasion has been suggested (13). The Ln-5 content in OSCC BM was recently quantified by confocal immunofluorescence imaging indicating a grading-dependent decrease of Ln-5 in the invasive front, whereas in re-established BM structures nearly normal Ln-5 levels could be found (14).

The extracellular glycoprotein Tn-C is composed of six disulphide-linked subunits. Isoforms are generated by alternative splicing within nine fibronectin type III homology repeats of the primary Tn-C mRNA, called domains A1–A4, B, AD1/2, C and D (15). The two main, quantitative important, variants arise by complete

Correspondence: Alexander Berndt, Institute of Pathology, Friedrich Schiller University, Ziegelmühlenweg 1, D-07743 Jena, Germany. Tel: +49 3641 933624, Fax: +49 3641 933111, E-mail: alexander.berndt@med.uni-jena.de

Accepted for publication August 14, 2006

inclusion or omission of the whole alternatively spliced region and are known as the small and the large isoform (further abbreviated Tn-C_S and Tn-C_L). In contrast to physiological adult tissues, where expression of Tn-C_L only rarely occurs, high expression levels can be detected in embryogenesis and during several processes of ECM remodelling including tumour progression (16–18). In OSCC, Tn-C_L mRNA has been specifically detected in carcinoma cells at the site of tumour invasion and the protein is deposited in the carcinoma stroma possibly contributing to enhanced tumour cell migration (17, 19).

Our group has previously described an interaction of Tn-C_L and Ln-5 in OSCC *in vitro* and *in situ*. Ln-5 and Tn-C_L show a similar pattern of distribution in the process of malignant progression in OSCC. Moreover, they functionally interact during the formation of an invasion-promoting extracellular tumour microenvironment. *In situ* different patterns of co-localization and co-deposition of both proteins could be detected by immunofluorescence double labelling and confocal laser scanning microscopy (CLSM; 20, 21). Especially dot-like co-depositions of Ln-5/ γ 2-chain and Tn-C_L in the ECM near ruptured BM and ribbon-like co-localization of both proteins in re-established BM structures seemed to be biologically meaningful within the process of tumour progression. Carter et al. reported on the regular formation of BM structures containing collagen type IV in OSCC (22). Ln-5 is the main protein of the anchoring filaments of BM and can be considered as a characteristic constituent even of reorganized BM structures occurring in OSCC (5, 6). Because Tn-C is known to modulate cellular adhesion to matrix proteins (16, 18), knowledge on the dynamic of Tn-C_L inclusion into re-established OSCC BM structures may contribute to the understanding of OSCC invasion and progression. Therefore, we have investigated the amount of BM included Tn-C_L in pre-malignant oral lesions as well as in oral carcinomas of different malignancy grade by CLSM-based quantitative co-localization analysis. Because Ln-5 is a main constituent of BM, the co-localization with Tn-C_L represents the extent of Tn-C_L that is involved in structural composition of reorganized OSCC BM.

Material and methods

Tissue material

For immunofluorescence double labelling and co-localization analysis, 38 surgical OSCC specimens of different malignancy grade (14 \times G1, 18 \times G2, 6 \times G3) and 18 specimens of normal, hyperplastic or dysplastic oral mucosa were available. The tissue specimens used in this study were derived from the Clinic of Maxillofacial Surgery of the Friedrich Schiller University of Jena. Ethical approval was obtained from the Local Research Ethic Committee. Fresh tissue blocks (4 \times 4 \times 4 mm) were shock frozen in isopropanol, cooled by liquid nitrogen and stored at a temperature of -75°C . Histopathological diagnosis was carried out on H&E-stained serial sections basing on the WHO classification of oral tumours and validated in the corresponding paraffin-

embedded tissue (23, 24). Cryostat sections of the frozen tissue samples were fixed in ice-cooled acetone for 15 min and subjected to immunofluorescence double labelling.

Double immunofluorescence labelling

To analyze the co-localization of Tn-C_L and the γ 2-chain of Ln-5 *in situ*, an immunofluorescence double labelling procedure using two monoclonal antibodies was performed. In a first step, 6 μm cryostat sections were incubated with the D4B5-antibody recognizing the γ 2-chain of Ln-5 (mouse-IgG₁, dilution 1:100; Chemicon International Inc., Temecula, CA, USA; 25). For detection of this primary antibody a Cy3-conjugated goat-antimouse immunoglobulin (Dianova, Hamburg, Germany) was applied. After thorough rinsing, sections were incubated with the biotinylated BC-3 antibody against Tn-C splicing variants containing domain B (mouse-IgG₁, dilution 1:500; source: L. Zardi and L. Borsi, Genoa, Italy; 26). The biotinylation of this antibody was undergone using the Animal Research Kit (DakoCytomation, Hamburg, Germany) following the manufacturer's instructions. Immunofluorescence detection of Tn-C_L was possible after subsequent incubation with FITC-conjugated streptavidin (DakoCytomation). To ensure reproducible and comparable staining results for quantitative co-localization analysis, the procedure was performed in a standardized way for all surgical specimens.

Immunofluorescence was analyzed by CLSM using a Zeiss microscope (LSM 510; Zeiss, Jena, Germany). An argon (488 nm) and a HeNe (543 nm) laser were combined with the light filters BP 505–530 and LP 560 (Zeiss). Multitrack detection of the fluorescence emission of both fluorochromes led to a two-channel image: channel 1 represented fluorescence of Cy3 (red) and channel 2 represented fluorescence of FITC (green; 27). By combining the pixel information of channels 1 and 2 it was possible to detect the overlapping Cy3 and FITC fluorescence signals: pixels with the information of both immunofluorescences (Cy3 and FITC) indicated a co-localization of the stained proteins (Ln-5 and Tn-C_L) which was displayed by a virtually generated colour (yellow). In contrast, co-deposition of both molecules led to separate fluorescence colour products. The double immunofluorescence labelling procedure including specificity controls has been recently described (21).

Quantitative co-localization analysis

For quantitative analysis of fluorescence immunolabelled Ln-5 (red), Tn-C_L (green) as well as co-localization of both molecules (yellow) in the BM region, the quantification tool of the LSM 510 Software Rel. 3.2 (Zeiss) was used. Inside the invasive area of one tumour section per case, five representative regions were chosen and each of them an image was generated by LSM using standardized conditions (magnification: 20 \times ; image-size: 230 \times 230 μm , A = 52 900 μm^2 ; constant LSM settings). Further, three arbitrary selected re-established BM regions within each of the five images were marked using a standardized ellipsoid drawing tool (defined

area: $A = \pi ab = 542.36 \mu\text{m}^2$; a and b represent the large and the small half-axis of the ellipse, an example is illustrated in Fig. 1e). By software-based calculative analysis the number of red (channel 1, Ln-5), green (channel 2, Tn-C_L) and yellow (channel 3, co-localization of both) pixels inside the defined areas of the drawing tools was calculated resulting in 15 pixel informations per channel for each tumour section. Averaging of these data led to a valid median value

representing the amount of the immunofluorescence-labelled structures (Ln-5, Tn-C_L and co-localization of both) in the BM regions of interest in each section.

Statistics

The correlation of the median of the number of co-localized pixels (yellow) with the histological grade (Bryne invasive front grading) was evaluated according to Kruskal–Wallis. A P -value of <0.05 was regarded to

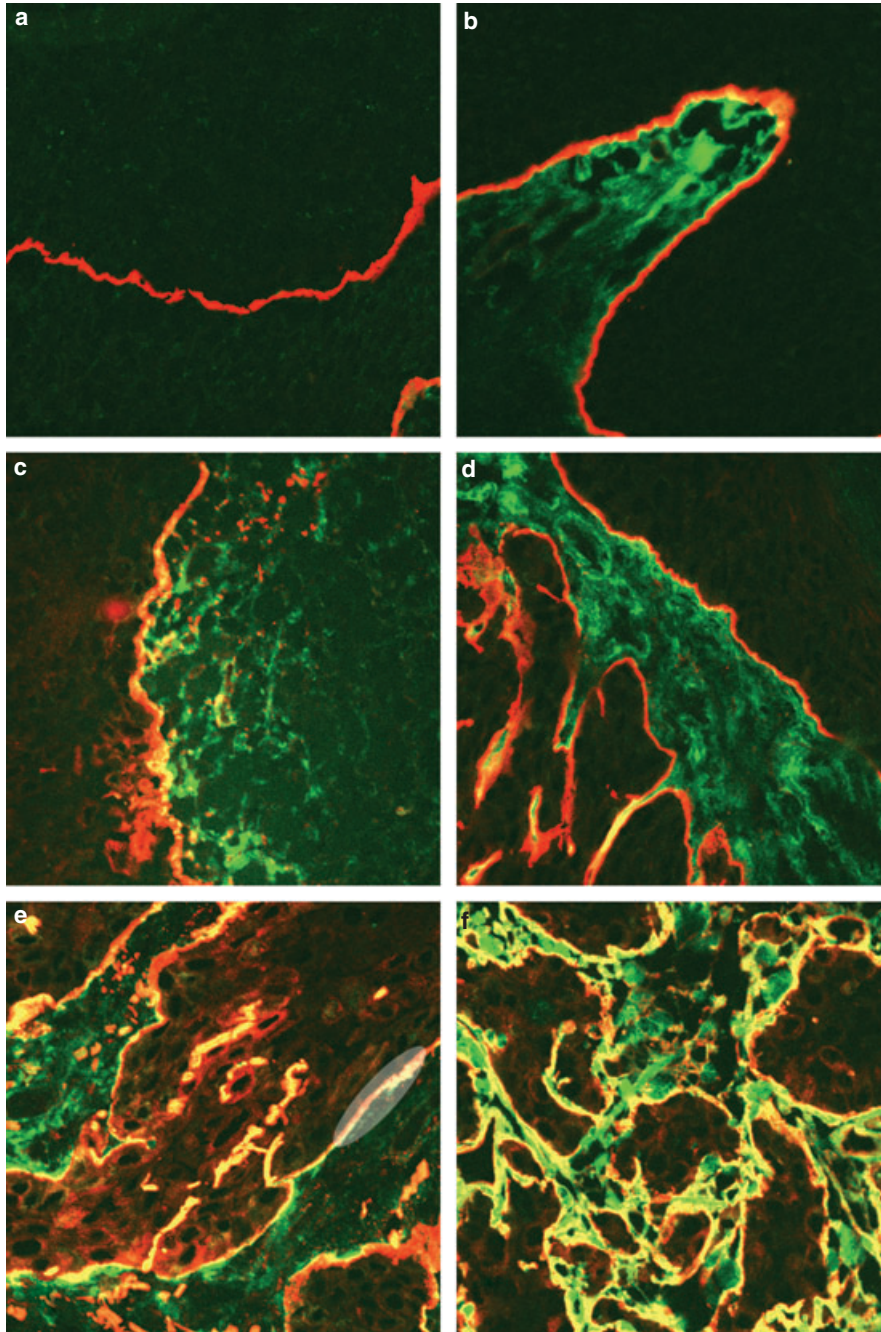


Figure 1 Immunofluorescence double labelling of Tn-C_L (green, clone BC-3) and Ln-5/γ2 (red, clone D4B5) for laser scanning microscopy-based co-localization analysis. In normal oral mucosa (a) no Tn-C_L is detectable and the basement membrane (BM) shows a continuous fluorescence immunostaining for Ln-5/γ2, whereas hyperplastic oral mucosa exhibits extracellular-deposited Tn-C_L exclusively in the subepithelial connective tissue (b). In dysplastic oral mucosa low levels of Tn-C_L could also be detected in the BM region indicated by the yellow colour (c). Furthermore, there is a significant increase of co-localized Tn-C_L and Ln-5/γ2 (yellow colour) in BM from G1 to G3 carcinomas [G1 (d), G2 (e), G3 (f)] indicating an increase of Tn-C_L incorporation into reorganized BM structures with rising malignancy grade. Scaling of all images: $0.45 \times 0.45 \mu\text{m}$.

be statistically significant. The analysis was performed using the SPSS software (Microsoft, San Antonio, CA, USA).

Results

Tn-C_L in the BM region of normal, hyperplastic and dysplastic oral mucosa

After double immunolabelling of Tn-C_L and the γ 2-chain of Ln-5, the BM region of normal oral mucosa showed no co-localization of both proteins indicating that there is no Tn-C_L arrangement in these areas (Fig. 1a). In hyperplastic oral mucosa regularly a subepithelial Tn-C_L-deposition can be observed but there was only a very low detection level of co-localization in the BM (Fig. 1b). In the stage of dysplasia a distinct extracellular deposition of Tn-C_L as well as occasional ribbon-like co-localization patterns in the ruptured BM could be revealed (Fig. 1c).

Co-localization of Tn-C_L and the Ln-5/ γ 2-chain in the BM region of OSCC

Basement membrane regions of OSCCs exhibited a linear ribbon-like co-localization pattern of Tn-C_L and the γ 2-chain of Ln-5. These reorganized BM occurred particularly around larger tumour cell clusters within the invasive front of the carcinomas. The extent of co-localization (yellow colour) revealed the Tn-C_L exclusively rearranged into the BM. At the site of carcinoma cells, a linear immunostaining for Ln-5 was detectable (red colour). In the extracellular matrix opposite to the carcinoma cells, Tn-C_L depositions (green colour) occurred and sometimes revealed a fibrillar staining pattern (Fig. 1d–f).

Quantification of the Tn-C_L extent arrangement in reorganized BM in OSCC

The amount of Tn-C_L included in the BM of OSCCs exhibiting different grades of malignancy as well as of normal, hyperplastic and dysplastic oral mucosa was determined by CLSM-based co-localization analysis, resulting in the total number of co-localized yellow pixels, and was correlated with the malignancy grade. The pixel intensity for Ln-5/ γ 2 alone was separately

assessed. The results are given in Table 1 showing the median of all medians of the sections per group. To give an impression of the variation within each group the minimum and maximum values of that medians are also presented. Whereas the amount of Ln-5/ γ 2 showed no significant differences within hyperplastic, dysplastic and re-established carcinomatous BM, Tn-C_L incorporation revealed a statistically significant increase with raising malignancy grade. The medians of co-localized pixels in normal and hyperplastic oral mucosa were very low (7.62 and 45.39). Compared with that, dysplastic mucosa showed higher levels of co-localized (yellow) pixels (161.02 pixels). In OSCC, the amount of co-localized pixels (yellow) depended on the malignancy grade. Morphologically, in well-differentiated G1 carcinomas, BM exhibited only a strict and discontinuous co-localization line of Tn-C_L and Ln-5/ γ 2 within the BM, whereas in moderately differentiated carcinomas (G2) a continuous and stronger co-localization pattern was detectable. Carcinomas that are poorly differentiated (G3) showed a wide ribbon of the co-localized proteins (Fig. 1d–f). CLSM-based quantitative co-localization analysis of well (G1) and moderately (G2) differentiated carcinomas led to medians of 3208 and 5063.3 yellow pixels, respectively. Poorly differentiated carcinomas (G3) revealed a median of 6505.7 co-localized (yellow) pixels. The increase of co-localized pixels in BM structures significantly correlated with an increasing malignancy grade (grade 1 vs. grade 3, $P = 0.003$). Differences in the median of co-localized pixels between histological grades 1 and 2 ($P = 0.005$), as well as 1 and 3 ($P = 0.002$) were statistically significant whereas medians between grades 2 and 3 showed no statistical significance ($P = 0.689$; Table 1).

Discussion

During tumour invasion, the large unspliced variant of Tn-C_L and the γ 2-chain of Ln-5 take part in the process of ECM reorganization. An increased expression of both proteins in the surrounding of OSCC cells *in vitro* and *in situ* has been shown by several authors (13, 17, 19, 28–30). The interaction and complex formation of Tn-C_L and Ln-5/ γ 2 in fibroblast/OSCC co-cultures as

Table 1 Results of confocal laser scanning microscopy (CLSM)-based quantitative analysis of Tn-C_L and Ln-5 co-localization (yellow pixels) and Ln-5 (red pixels) in basement membrane structures of normal, hyperplastic and dysplastic oral mucosa as well as oral squamous cell carcinomas of different malignancy grade

Cases	Grading	Co-localized pixels (median \pm SD)	Medians of co-localized pixels (maximum)	Medians of co-localized pixels (minimum)	Ln-5 (red) pixels (median \pm SD)	Medians of Ln-5 (red) pixels (maximum)	Medians of Ln-5 (red) pixels (minimum)
6	Normal	0.5 \pm 2.4	7	0	410.5 \pm 110.8	616	303
6	Hyperplastic	7 \pm 42.6	97	0	276 \pm 89.2	490	254
6	Dysplastic	117 \pm 109.5	343	42	287.5 \pm 111.4	484	178
14	G1	184.5 \pm 78.7* ***	381	75	288 \pm 69.2	461	86
18	G2	318.5 \pm 94.6* **	452	56	269.5 \pm 129.8	661	34
6	G3	412.5 \pm 72** ***	472	264	307.5 \pm 95	452	237

Values are presented as medians of all medians of the sections per group. Furthermore, the variation within each group is represented by the maximum and minimum values of that medians.

* $P = 0.005$, ** $P = 0.689$, *** $P = 0.003$.

well as different co-localization and co-deposition patterns *in situ* in dependence on localization within the tumour have been recently described by our group (20, 21). Carter et al. reported on an invasion-associated formation of reorganized BM structures in OSCC (22). Because Ln-5 is the main protein of the anchoring filaments of BM and realizes its connection to the hemidesmosome of the cell it can be considered as a characteristic constituent even of reorganized BM structures occurring in OSCC (5, 6).

A subepithelial, ribbon-like immunostaining for Tn-C in hyperplastic and mild dysplastic oral mucosa was recently demonstrated (28). Häkkinen et al. described an immunostaining for Tn-C_L in the subepithelial connective tissue of oral mucosa using the antibody BC-2 against the A1/A4 splicing domains of the molecule (26, 31). In contrast, in our present study using the antibody BC-3 against the B domain-containing Tn-C variants in normal oral mucosa nearly no subepithelial deposits of Tn-C_L could be observed. This discrepancy may be explained by a differential expression of splicing domains. Indeed, B and/or D domain-containing Tn-C was suggested as a predictor for invasion in breast cancer (32).

Description of an increased expression of Tn-C in oral carcinoma *in situ* led to the suggestion that it might play an important role in early stages of OSCC tumour progression (29). We previously observed a ribbon-like co-localization pattern of Tn-C_L and Ln-5/ γ 2 in reorganized OSCC BM structures not occurring in normal oral mucosa (21). To our knowledge, informations on quantitative changes in BM incorporated Tn-C_L during carcinoma development are not available as yet.

Applying a CLSM-based quantification of protein co-localization, we are able to assess the relative amount of interacting BM proteins. The double immunofluorescence labelling with Ln-5/ γ 2 enables the detection of Tn-C_L exclusively incorporated in the reorganized BM that can be therefore quantitatively evaluated. Because of the relatively constant amount of Ln-5/ γ 2 in the scanned reorganized BM structures, an increased co-localization indeed represents an increased incorporation of Tn-C_L in the re-established OSCC BM structures. Our findings of comparable Ln-5/ γ 2 levels in hyperplastic, dysplastic and in re-established carcinomatous BM supports the findings of Haas et al. reporting on nearly 'normal' Ln-5/ γ 2 values in re-established BM in more central tumour parts (14). In this study, for the quantification of Ln-5, the antibody GB3 was used that recognizes the γ 2-chain only assembled with the other chains into the Ln-5 heterotrimer (33). In contrast, the antibody D4B5, used in our study, binds to all γ 2-chains independent on its association with other Ln chains and therefore represents the whole amount of γ 2-chain in the re-established BM (34). Differences in the detection level of Ln-5 between both studies therefore depend on variations in Ln-5 chain assembly within OSCC BM structures. As also shown for normal colonic mucosa, colonic adenomas and carcinomas with different antibodies against

the α 3-, β 3- and γ 2-chains (35), the γ 2-chain at all showed the lowest variations in the BM staining intensity between different parts of the lesion and is therefore a good marker for reorganized BM structure decoration.

However, our results indicate that reorganized BM are not normal ones but differ in the content of oncofetal matrix protein variants. This structural phenomenon is suggested to represent a specialized form of an OSCC BM whose occurrence, in quality and quantity, depends on the localization within the tumour as well as on its biological behaviour. The results of the present study clearly evidence for the first time the existence of a correlation between the extent of Tn-C_L-Ln-5/ γ 2 co-localisation in re-established BM structures and malignancy grade in OSCC. Because the malignancy grade represents tumour cell dedifferentiation and the invasive pattern, the increased amount of Tn-C_L should be relevant for the biological behaviour of the tumour.

Broll et al. also reported on a discontinuous tenascin immunostaining close to the BM in highly differentiated tumours of the oesophagus, small intestine and colorectum using an antibody against all tenascin-C variants. But, in contrast to our results for OSCC, any correlation of tenascin deposition patterns to the malignancy grade could not be established (36). This indicates that especially Tn-C_L must play a major role during the invasion-associated reorganization of OSCC BM. It is known that the large, unspliced form of Tn-C is a cell adhesion-modulating molecule that is particularly expressed in the ECM during the processes of tissue remodelling (36, 37). It shows a high sensitivity for matrix degradation enzymes contributing to higher level of ECM flexibility (38). Because the reorganization of BM in invasive OSCC was suggested as a preservative for normal function of squamous epithelia, our results indicate that the arrangement of Tn-C_L into the BM is a step to higher flexibility of that specialized ECM structure and is supposed to be a presupposition for BM disintegration during OSCC growth and invasion (22).

References

1. Kosmehl H, Berndt A, Katenkamp D. Molecular variants of fibronectin and laminin: structure, physiological occurrence and histopathological aspects. *Virchows Arch* 1996; **42**: 311–22.
2. Engbring JA, Kleinman HK. The basement membrane matrix in malignancy. *J Pathol* 2003; **200**: 465–70.
3. Katayama M, Sekiguchi K. Laminin-5 in epithelial tumour invasion. *J Mol Histol* 2004; **35**: 277–86.
4. Aumailley M, Bruckner-Tuderman L, Carter WG, et al. A simplified laminin nomenclature. *Matrix Biol* 2005; **24**: 326–32.
5. Rousselle P, Lunstrum GP, Keene DR, Burgeson RE. Kalinin: an epithelium-specific basement membrane adhesion molecule that is a component of anchoring filaments. *J Cell Biol* 1991; **114**: 567–76.
6. Masunaga T, Shimizu H, Ishiko A, et al. Localization of laminin-5 in the epidermal basement membrane. *J Histochem Cytochem* 1996; **44**: 1223–30.

7. Meneguzzi G, Marinkovich MP, Aberdam D, Pisani A, Burgeson R, Ortonne JP. Kalinin is abnormally expressed in epithelial basement membranes of Herlitz's junctional epidermolysis bullosa patients. *Exp Dermatol* 1992; **1**: 221–9.
8. Miyazaki K, Kikkawa Y, Nakamura A, Yasumitsu H, Umeda M. A large cell-adhesive scatter factor secreted by human gastric carcinoma cells. *Proc Natl Acad Sci U S A* 1993; **90**: 11767–71.
9. Ryan MC, Tizard R, VanDevanter DR, Carter WG. Cloning of the LamA3 gene encoding the alpha 3 chain of the adhesive ligand epiligrin. Expression in wound repair. *J Biol Chem* 1994; **269**: 22779–87.
10. Vailly J, Verrando P, Champlaud MF, et al. The 100-kDa chain of nicein/kalinin is a laminin B2 chain variant. *Eur J Biochem* 1994; **219**: 209–18.
11. Pyke C, Rømer J, Kallunki P, et al. The γ 2 chain of kalinin/laminin 5 is preferentially expressed in invading malignant cells in human cancers. *Am J Pathol* 1994; **145**: 782–91.
12. Pyke C, Salo S, Ralfkiær E, Rømer J, Danø K, Tryggvason K. Laminin-5 is a marker of invading cancer cells in some human carcinomas and is coexpressed with the receptor for urokinase plasminogen activator in budding cancer cells in colon adenocarcinomas. *Cancer Res* 1995; **55**: 4132–9.
13. Kosmehl H, Berndt A, Strassburger S, et al. Distribution of laminin and fibronectin isoforms in oral mucosa and oral squamous cell carcinoma. *Br J Cancer* 1999; **81**: 1071–9.
14. Haas KM, Berndt A, Stiller KJ, Hyckel P, Kosmehl H. A comparative quantitative analysis of laminin-5 in the basement membrane of normal, hyperplastic, and malignant oral mucosa by confocal immunofluorescence imaging. *J Histochem Cytochem* 2001; **49**: 1261–8.
15. Mighell AJ, Thompson J, Hume WJ, Markham AF, Robinson PA. Human tenascin-C: identification of a novel type III repeat in oral cancer and of novel splice variants in normal, malignant and reactive oral mucosae. *Int J Cancer* 1997; **72**: 236–40.
16. Borsi L, Carnemolla B, Nicolo G, Spina B, Tanara G, Zardi L. Expression of different tenascin isoforms in normal hyperplastic and neoplastic human breast tissues. *Int J Cancer* 1992; **52**: 688–92.
17. Hindermann W, Berndt A, Borsi L, et al. Synthesis and protein distribution of the unspliced large tenascin-C isoform in oral squamous cell carcinoma. *J Pathol* 1999; **189**: 475–80.
18. Bosman FT, Stamenkovic I. Functional structure and composition of the extracellular matrix. *J Pathol* 2003; **200**: 423–8.
19. Ramos DM, Chen BL, Boylen K, et al. Stromal fibroblasts influence oral squamous-cell carcinoma cell interactions with tenascin-C. *Int J Cancer* 1997; **72**: 369–76.
20. Berndt A, Borsi L, Hyckel P, Kosmehl H. Fibrillary co-deposition of laminin-5 and large unspliced tenascin-C in the invasive front of oral squamous cell carcinoma *in vivo* and *in vitro*. *J Cancer Res Clin Oncol* 2001; **127**: 286–92.
21. Franz M, Hansen T, Richter P, et al. Complex formation of the laminin-5 γ 2 chain and large unspliced tenascin-C in oral squamous cell carcinoma in vitro and in situ: implications for sequential modulation of extracellular matrix in the invasive tumor front. *J Histochem Cell Biol* 2006; **126**: 125–31.
22. Carter RL, Burman JF, Barr L, Gusterson BA. Immunohistochemical localization of basement membrane type IV collagen in invasive and metastatic squamous carcinomas of the head and neck. *J Pathol* 1985; **147**: 159–64.
23. Bryne M, Koppang HS, Lilleng R, Kjaerheim A. Malignancy grading of the deep invasive margins of oral squamous cell carcinoma has high prognostic value. *J Pathol* 1992; **166**: 375–81.
24. Pindborg JJ, Reichart PA, Smith CJ, van der Wal I. *Histological typing of cancer and precancer of the oral mucosa*/World Health Organization. Berlin: Springer, 1997.
25. Mizushima H, Koshikawa N, Moriyama K, et al. Wide distribution of laminin-5 gamma 2 chain in basement membranes of various human tissues. *Horm Res* 1998; **50** (Suppl. 2): 7–14.
26. Balza E, Siri A, Ponassi M, et al. Production and characterization of monoclonal antibodies specific for different epitopes of human tenascin. *FEBS Lett* 1993; **332**: 39–43.
27. Manders EMM, Verbeek FJ, Aten JA. Measurement of colocalization of objects in dual-colour confocal images. *J Microsc* 1992; **169**: 375–82.
28. Tiitta O, Happonen RP, Virtanen I, Luomanen M. Distribution of tenascin in oral premalignant lesions and squamous cell carcinoma. *J Oral Pathol Med* 1994; **23**: 446–50.
29. Ramos DM, Chen B, Regezi J, Zardi L, Pytela R. Tenascin-C matrix assembly in oral squamous cell carcinoma. *Int J Cancer* 1998; **75**: 680–7.
30. De Wever O, Mareel M. Role of tissue stroma in cancer cell invasion. *J Pathol* 2003; **200**: 429–47.
31. Häkkinen L, Hildebrand HC, Berndt A, Kosmehl H, Larjava H. Immunolocalization of tenascin-C, α 9 integrin subunit, and α 6 β 4 integrin during wound healing in human oral mucosa. *J Histochem Cytochem* 2000; **48**: 985–98.
32. Adams M, Jones JL, Walker RA, Pringle JH, Bell SC. Changes in tenascin-C isoform expression in invasive and preinvasive breast disease. *Cancer Res* 2002; **62**: 3289–97.
33. Matsui C, Nelson CF, Hernandez GT, Herron GS, Bauer EA, Hoeffler WK. γ 2 Chain of laminin-5 is recognized by monoclonal antibody GB3. *J Invest Dermatol* 1995; **105**: 648–52.
34. Koshikawa N, Moriyama K, Takamura H, et al. Overexpression of laminin gamma 2 chain monomer in invading gastric carcinoma cells. *Cancer Res* 1999; **59**: 5596–601.
35. Sordat I, Bosman FT, Dorta G, et al. Differential expression of laminin-5 subunits and integrin receptors in human colorectal neoplasia. *J Pathol* 1998; **185**: 44–52.
36. Broll R, Meyer S, Neuber M, Bruch HP. Expression of tenascin in tumors of the esophageus, small intestine and colorectum. An immunohistochemical study. *Gen Diagn Pathol* 1995; **141**: 111–9.
37. Murphy-Ullrich JE, Lightner VA, Aukhil I, Yan YZ, Erickson HP, Hook M. Focal adhesion integrity is downregulated by the alternatively spliced domain of human tenascin. *J Cell Biol* 1991; **115**: 1127–36.
38. Siri A, Knäuper V, Veirana N, Caocci F, Murphy G, Zardi L. Different susceptibility of small and large human tenascin-C isoforms to degradation by matrix metalloproteinases. *J Biol Chem* 1995; **270**: 8650–4.

Acknowledgements

The study was partially supported by the Thuringian Ministry of Science, Research and Art (ThMWFK) and IZKF of the University Jena (B307-04004), by the Associazione Italiana per la Ricerca sul Cancro (AIRC), and by the European Community (FP6, LSH-CT-2003-5032, STROMA; this publication reflects only the authors view. The European Commission is not liable for any use that may be made of the information contained).

This document is a scanned copy of a printed document. No warranty is given about the accuracy of the copy. Users should refer to the original published version of the material.